Mine Water Environ (2016) 35:55–63
DOI 10.1007/s10230-015-0346-4

TECHNICAL ARTICLE

Thallium Contamination in the Raibl Mine Site Stream Drainage System (Eastern Alps, Italy)

Riccardo Petrini[1] · Rosa Cidu[2] · Francesca F. Slejko[3]

Received: 15 September 2014 / Accepted: 5 May 2015 / Published online: 14 May 2015

Abstract The Raibl mine (Cave del Predil village, northern Italy) belongs to the Pb–Zn minerogenetic district in the southeastern Alps, hosted in Middle Triassic carbonates. The drainage water quality reflects the high acid-buffering capacity of the carbonate rocks, which controls the mobility of most metals. In particular, Fe is non-detectable in solution, having formed hydrous-oxides precipitates. Molybdenum, Ni, Zn, Cd, Pb, and Tl are present, and the Pb, Tl, and Zn concentrations sometimes exceed the Italian regulatory thresholds. Thallium concentrations substantially exceed the 2 µg/L limit at some sampling stations, ranging between 12 and 30 µg/L in the mine drainage, and reaching 5 µg/L downstream of the mine site, despite strong dilution. The data indicate that Tl behaves almost conservatively and is not significantly scavenged by the Fe precipitates. The elevated Tl represents a potential risk for the stream ecosystem. Although Tl is not regulated in drinking water in Italy or the European Community, its distribution in natural waters may help to determine if health actions should be taken.

Keywords Carbonate-hosted ores · Abandoned mines · Mine waters · Water contaminants

✉ Riccardo Petrini
riccardo.petrini@unipi.it

[1] Dipartimento di Scienze della Terra, Università di Pisa, Via S. Maria 53, 56123 Pisa, Italy

[2] Dipartimento di Scienze Chimiche e Geologiche, Università di Cagliari, Via Trentino 51, 09127 Cagliari, Italy

[3] Dipartimento di Matematica e Geoscienze, Università di Trieste, Via Weiss 8, 34127 Trieste, Italy

Introduction

A common legacy of mining can be metal-rich acidic mine drainage (AMD) and the release of toxic compounds to the receiving ecosystem (e.g. Nordstrom 2011). The mitigation of the environmental impact of metals and metalloids in AMD produced by sulfide mineral oxidation is of great environmental concern (Alderton et al. 2005; Cidu et al. 2012; Jambor et al. 2003). Although the acidity of mine drainage receives most of the attention, the primary sources of toxicity for the biota and humans are the dissolved and potentially toxic trace metals (e.g. Luoma and Rainbow 2008). Some of these can be elevated in higher pH-buffered drainages, such as those produced in deposits that form in platform carbonate sequences (e.g. Foley 2002), since the increases of pH and alkalinity that occur by calcite dissolution do not necessarily prevent metal leaching and transport in mine effluents (Plumlee et al. 1999). Whereas some metals, such as Fe, Al, and Cu are readily scavenged from the aqueous phase as the pH increases, other ionic species of element such as Sb, Cd, Zn, Mo, and Tl may remain in solution, with some reaching concentrations of hundreds of µg/L in waters draining mineralized areas (Cidu 2011; Nriagu 1998). In particular, Tl is hosted in base metal sulfides such as chalcopyrite, pyrite, galena, and sphalerite (Kelley et al. 2004; Martinez-Frías 1991; Murao and Itoh 1992; Nriagu 1998) up to wt% amounts. This Tl may be readily mobilized during oxidation of the sulfide minerals and transported into the ecosystem via water transport (Xiao et al. 2004).

In water, Tl occurs in two oxidation states, Tl(I) and Tl(III), whose relative stability depends on the pH and redox conditions. Tl(I) is thermodynamically more stable state at the conditions commonly found in natural waters (Kaplan and Mattigod 1998). It is mainly present as a free

ion in low ionic strength water; otherwise, it may form complexes with halogens, oxygen, and sulfur. Tl(I) also complexes with hydroxide, carbonate, and sulfate ligands, which are very soluble in water ($K_{sp} \approx 10^{-3.7}$ at 25 °C; Sager 1994). It has been observed that compared with other trace elements (e.g. As, Cd, Co, Cr, Cu, Ni, Pb, Zn), Tl has a low affinity for suspended particles and undergoes little removal by conventional (hydroxide precipitation) treatment of mine water (Law and Turner 2011). Only under very reducing conditions will Tl precipitate as Tl_2S sulfide, though in very strongly oxidizing environments, Tl(III) may precipitate as $Tl(OH)_3$. Furthermore, Tl(I) seems not to be strongly complexed by humic acids in soils: this implies that under some circumstances, significant amount of Tl can move from soil to pore waters and plants, becoming mobile in the environment and bio-available. However, the association of Tl with Mn oxides with a low pH point of zero charge has been demonstrated; this has been explained by the further oxidation of Tl(I) to Tl(III) while Mn(IV) reduces to Mn(II), forming Tl_2O_3 precipitates (Bidoglio et al. 1993; Koschinsky and Hein 2003) that can collect in water pipes during scaling (ATSDR 2014). Whilst mining activity at Raibl ceased in 1990, the archeology of mining is preserved and part of the mine is now open to visitors. The environmental impact of the Raibl mine drainage, including the trace level occurrence of potentially toxic elements, has not been previously addressed.

In this study, trace elements, major ion chemistry, and physic-chemical properties were measured in some of the drainages and stream water from the mine site. The behavior of Tl, which it is known to be highly toxic to humans and biota (e.g. Mulkey and Oehme 1993; Peter and Viraraghavan 2005), is a particular focus.

The Raibl Mine Site

The Raibl mine (Cave del Predil village, northern Italy) belongs to the Pb–Zn minerogenetic district in the southern Alps (Fig. 1) (Ebner et al. 2000 and references therein). Raibl is a Pb–Zn complex hosted in Middle Triassic carbonates, which cover the metamorphic basement and are aligned along the Periadriatic lineament (Cerny 1989). Mineralization is usually stratabound within the Carnian, and to a lesser extent, Ladinian sediments, and has been classified as Bleiberg-type (Brigo and Omenetto 1979) or Alpine-type, a subclass of the low-temperature Pb–Zn carbonate deposits (Schroll 1996), having many features in common with the Mississippi Valley-type Pb–Zn deposits (Leach et al. 2005, 2010), including the Ge-Tl-As association (Leach et al. 1995). The dominant mineral assemblage is constituted by sphalerite, galena, pyrite, marcasite, dolomite, calcite, and quartz, with hypothesized crustal sources for metals. The genesis of the Alpine-type Pb–Zn deposits in the eastern and southern Alps is, however, still controversial (Schroll 1996; Schroll and Prochaska 2004).

The Raibl Pb–Zn deposit is located within a dolostone formation of Middle-Upper Triassic age, more than 1000 m thick, with intercalations of bituminous limestones; the ores are linked to N–S and NE–SW fault systems (Brigo and Omenetto 1979; Brigo et al. 1977), along

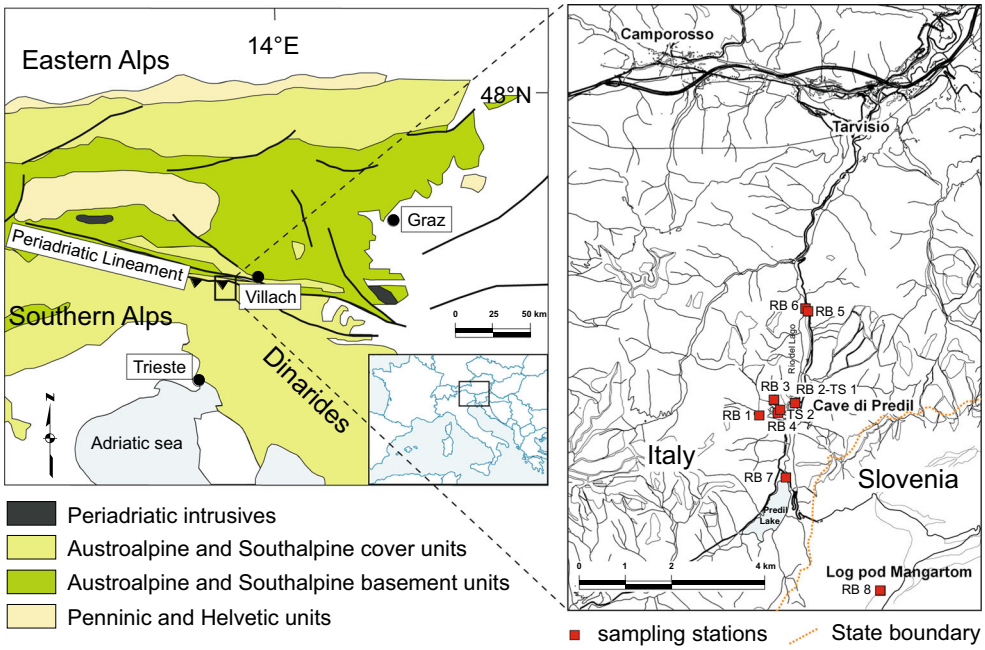

Fig. 1 Simplified geological map (modified after Schroll and Rantitsch 2005) and locations of the sampling stations

which the mineralizing solutions replaced limestone. Ore-bearing beds are made by marls intercalated by carbonates. The fundamental mineral association consists of sphalerite, galena, and pyrite, with lesser amounts of barite and fluorite. Minor phases are anglesite, bianchite, cerussite, goslarite, hydrozincite, jordanite, melanterite, smithsonite, and wulfenite. The Pb/Zn ratio ranges between 1 and 0.1 (Schroll 1996).

The Raibl mine complex contains about 110 km of galleries, from 600 m below ground level to 500 m above. The mine was closed in 1991. During 2008–2009, the dewatering system was shut down and the mine gradually flooded, forming a large aquifer in the extracted mine voids, with high porosity and hydraulic conductivity. The phreatic water table, with a nearly uniform hydraulic head, is controlled by a horizontal baseflow through a gallery about 4.8 km in length (called the Bretto gallery) at 260 m below ground level, which represents a major drainage of the mine pool; the flow ranges from 250 to 300 L/s. The Bretto gallery discharges directly into the Soča River, in Slovenia. Effluents from galleries above the ground level discharge into the Rio Del Lago stream (Fig. 1), which flows near the mine site and by a mine waste rock dump before becoming a tributary of the Drava and Danubio rivers.

Precipitation in the area is linked to the interaction of airflow patterns and relief, and water resources are provided by both rainfall and snow. Autumn is usually the wettest season, and winter and summer the driest.

Sampling and Analytical Methods

Water samples were collected for the present study during a November 2010 survey (Fig. 1). Two samples from upstream and downstream of the mine site (RB7 and RB5, respectively) represented the Rio del Lago River during median-flow conditions. One sample (RB6) was collected in static mode from a shallow-depth piezometer sampling shallow sub-riverbed water, close to the RB5 sampling station. Two samples represent mine drainages, from the ground level system of galleries collecting infiltration from the unsaturated zone (sample RB2) and from the Bretto gallery, in Slovenia (sample RB8). Two samples were from natural springs in the mineralized area (RB3 and RB4). One sample represents a small outflow of sulfurous water within a mine gallery (sample RB1). Also, two water samples were taken in a preliminary survey during August 2006: one was from the ground level drainage (sample TS1, same station as RB2) and the other was from seepage in a ground level gallery (sample TS2). The average precipitation recorded by the local rain gauge network during Autumn—early Winter 2010 and Summer 2006 was 590 and 270 mm, respectively.

Water temperature, bulk redox potential (Eh), pH, and electrical conductivity (EC) were measured in the field during sampling. Accuracy was ±0.1 °C for temperature, ±0.05 for pH; ±0.01 V for Eh, and 1 % for EC. The measured Eh was reported relative to the standard hydrogen electrode using a ZoBell's solution (Nordstrom 1977) as a reference. Alkalinity was determined in the field by acidimetric titration with 0.1 N HCl and attributed to bicarbonate ions. Replicate analyses yielded an internal confidence of 5 %. Samples for chemical and isotopic analyses were stored in clean polyethylene containers. For major cations and trace element analyses, the water samples were filtered using a 0.45 μm nylon filter, and stabilized by adding ultrapure HNO_3. Major ions were determined by ion chromatography (Dionex ICS3000). Trace element concentrations were obtained by ICP-MS (PerkinElmer-DRCe instrument); the Rh internal standard was used to correct the ICP-MS instrumental drift. Analytical error was estimated by analysis of the certified SRM1643e solution supplied by the NIST (Gaithersburg, Maryland, USA); diluted samples were analyzed to check for matrix interferences, and field blanks were analyzed to detect procedural contamination. The Sr isotopic composition was measured on filtered samples using a VG Micromass 54E thermal ionization mass spectrometer (TIMS), after conventional chemical separation from the matrix. The measured $^{87}Sr/^{86}Sr$ ratios were fractionation-corrected to $^{86}Sr/^{88}Sr = 0.1194$ by international convention. Repeated analyses of the SRM-987 standard gave an average $^{87}Sr/^{86}Sr$ ratio of 0.71024 ± 0.00002 (n = 25), and no correction was applied to the measured isotopic ratio for instrumental bias. Errors represent in-run statistics at $2 - \sigma$ confidence level. Chemical speciation calculations were performed using the PHREEQC code (Parkhurst and Appelo 1999) and the MINTEQ database (Allison et al. 1991).

Results and Discussion

The physic-chemical parameters and the major ion chemistry are reported in Table 1. The pH ranges between 7.8 and 8.3, indicating the dominance of the bicarbonate source throughout this region; the higher pH value was measured in the Rio del Lago upstream of the mine site, and is consistent with waters equilibrated with calcite and atmospheric CO_2. The bulk Eh ranges between 0.32 and 0.48 V, except for water sample RB1, which represented the only known sulfurous anoxic drain within the mine galleries and likely reflected the role of organic oxidizable matter that occurs as intercalations of dark bituminous layers within the carbonates.

The river and shallow sub-riverbed ECs ranged from 180 to 190 μS/cm. The drainages and groundwater were more saline. In particular, samples collected during the

Table 1 Physico-chemical parameters and major ion data (in mg/L)

Sample	2010 Survey								2006 Survey	
	RB1 Mine gallery	RB2 Drainage	RB8 Drainage	RB3 Natural spring	RB4 Natural spring	RB5 Down-stream	RB6 = RB5	RB7 Upstream	TS1 = RB2	TS2 Mine gallery
T (°C)	10.5	10.3	9.2	17.8	10.1	10.9	11.1	20.7	12.5	11.4
Eh (V)	0.00	0.39	0.37	0.36	0.37	0.36	0.35	0.32	0.44	0.48
pH	7.9	8.1	8.1	8.2	8.1	8.0	8.0	8.3	8.2	7.8
EC (µS/cm)	320	327	250	279	271	190	189	180	610	1980
F	1.27	0.12	0.10	0.01	0.09	0.02	0.01	0.02	0.06	1.47
Cl	0.53	0.63	1.45	0.71	0.54	1.51	1.22	0.81	0.84	73
NO_2	<0.01	0.015	<0.01	<0.01	<0.01	<0.01	<0.01	0.025	<0.01	nd
NO_3	0.56	1.61	2.11	3.50	3.17	1.98	1.73	1.92	1.3	nd
PO_4	<0.1	<0.1	<0.1	<0.1	<0.1	<0.1	<0.1	<0.1	nd	nd
SO_4	17.53	81.70	35.69	4.52	65.15	5.32	5.60	1.06	190	900
HCO_3	207	165	122	226	146	134	134	128	140	96
Na	1.59	0.60	1.80	1.53	0.092	1.12	0.94	0.50	1.6	4.2
NH_4	0.18	0.11	<0.01	<0.01	<0.01	<0.01	<0.01	<0.01	nd	nd
K	2.30	0.41	2.11	3.60	1.85	0.19	0.20	0.09	2.5	112
Mg	23.12	21.56	12.94	1.14	11.79	9.96	9.17	9.83	31	74
Ca	37.0	52.6	37.3	70.5	53.9	31.1	37.8	30.6	84	274

nd not determined

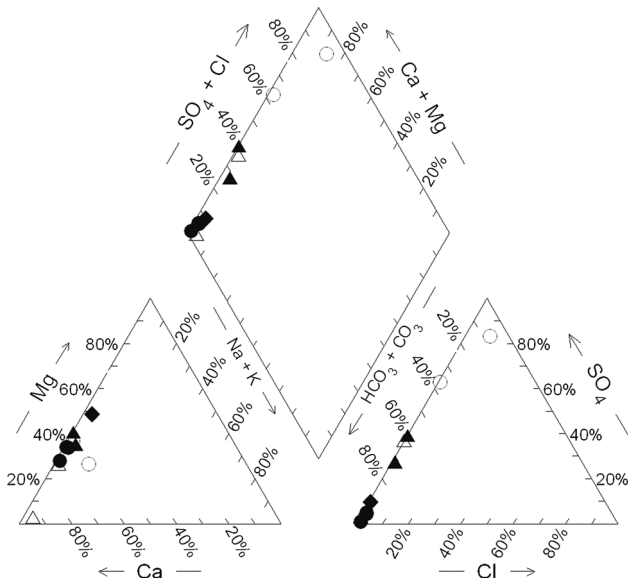

Fig. 2 Piper diagram for the studied samples. Symbols are: *filled triangle*: drainages; *open triangle*: springs; *diamond*: sulfurous spring; *filled circle*: river and sub-riverbed waters; *open circle*: drainages, 2006 survey

summer of 2006 (TS1 and TS2) had EC values of 610 and 1980 µS/cm, respectively.

In the Piper plot (Fig. 2), the major anions (Cl^-, SO_4^{2-}, HCO_3^-) and cations (Mg^{2+}, Ca^{2+}, Na^+, K^+) indicate that the stream and sub-riverbed samples (RB5, RB7, and RB6, respectively) belong to the Ca-HCO_3 type. Groundwater (samples RB3 and RB4) ranged from Ca-HCO_3 to the Ca–Mg-HCO_3 type. Drainages and the seepage from a gallery ceiling (samples RB1, RB8, TS1, and TS2, respectively) belong to the Ca–Mg–SO_4 and Ca–Mg–SO_4–Cl hydrofacies, and are shifted towards a relative increase in the sulfate content. In particular, sample TS2 is characterized by a high EC and markedly higher Cl^-, SO_4^{2-}, Na^+, K^+, Ca^{2+}, and Mg^{2+} content with respect to the remaining water (Table 1), probably due to long water–rock interaction.

The SO_4 and Ca increase in sample TS2 in particular likely reflects gypsum dissolution, initially precipitated as a secondary mineral during limestone neutralization of the sulfate-rich AMD, according to:

$$CaCO_3 + H_2SO_4 + H_2O \rightarrow CaSO_4 \cdot 2H_2O + CO_2$$

Water hardness, expressed as the equivalent concentration of $CaCO_3$, ranged between 76 mg/L in TS2 to 187 mg/L in RB3; the average value was 121 mg/L. This parameter influences the toxicity of metals in aquatic ecosystems since higher Ca concentrations tend to be protective by competing with metals for binding sites on the surfaces of cells. Thus, higher concentrations than indicated by default water quality guideline values may be able to be tolerated by organisms in Ca-rich waters (Smith and Huyck 1999).

Trace element data (Table 2) show that Be, V, Cr, Se, Ag, Te, Hg, and Bi were invariably below the detection limits. Dissolved Fe was also non-detectable, as expected, since it forms hydrous-oxide precipitates at the pH and sulfate content measured in these waters. Widespread encrustations of Fe hydroxides were visible as coatings on the limestone fragments in the waste pile. Iron hydroxide may act as a scavenger for other metals and metalloids. In particular, As remains at low concentration in most samples (from below detection limit to 1.8 μg/L), with the exception of RB2, where it reached the 10 μg/L concentration threshold imposed by Italian Regulations (decree 152/2006). Other trace elements show a large concentration range; in particular, Ni, Zn, Cd, Pb, and Tl in some samples exceeded the maximum admissible concentrations of 20, 3000, 5, 10, and 2 μg/L, respectively. It has to be noted that Mo reached 330 μg/L in sample TS1 and that a Tl concentration of 11.6 μg/L was measured in the Bretto gallery drainage (sample RB8), despite the effects of dilution. Concentrations of 30 and 6.8 μg/L Tl were measured in drainages RB2 and TS1 in 2010 and 2006, respectively, indicating a significant seasonal variability. The Tl concentration in the Rio del Lago stream downstream of the mine waste was 4.8 μg/L. Overall, these survey data indicate that Tl contamination may represent an environmental risk in the Raibl mine area.

Parental materials for Tl are usually sphalerite and pyrite. However, the low Tl concentration measured in water with the highest Zn content (sample TS2) suggests that sphalerite is not the main source for the released Tl. Preliminary analysis of pyrite from this location revealed significant Tl content (at the tens of ppm level), and pyrite oxidation could be the major source of Tl.

Table 2 Trace element analysis (μg/L) and $^{87}Sr/^{86}Sr$ isotope ratios

Sample	2010 Survey								2006 Survey	
	RB1	RB2	RB8	RB3	RB4	RB5	RB6	RB7	TS1	TS2
Li	4.8	0.6	2.8	15.4	1.3	0.37	0.36	0.1	3	1
Be	<0.5	<0.5	<0.5	<0.5	<0.5	<0.5	<0.5	<0.5	nd	nd
B	30	<10	<10	<10	12	<10	<10	<10	<10	<10
Al	50	30	30	50	40	30	50	40	<10	<10
V	<5	<5	<5	<5	<5	<5	<5	<5	<2	<2
Cr	<5	<5	<5	<5	<5	<5	<5	<5	<2	<2
Fe	<100	<200	<100	<200	<200	<100	<100	<100	<10	<10
Mn	0.6	0.4	0.52	<1	<1	<1	0.59	0.11	3	2
Ni	<1	6.9	<1	<1	<1	<1	<1	<1	29	7.1
Co	0.03	0.85	0.08	0.08	0.05	0.03	0.05	0.02	5.3	0.4
Cu	<1	0.3	<1	<1	<1	<1	1	<1	<1	15
Zn	<5	546	566	68	540	876	173	<1	600	6600
As	<1	9.7	1.8	1.6	0.3	1.5	0.7	<0.2	2	<1
Se	<5	<5	<5	<5	<5	<5	<5	<5	nd	nd
Rb	1.1	0.40	8.9	7.5	0.80	0.2	0.6	0.1	3	9
Sr	5620	119	177	718	178	86	60	13	570	200
Mo	2.6	152	18	3.3	5.6	1.3	1.2	0.4	330	1.2
Ag	<0.05	<0.05	<0.05	<0.05	<0.05	<0.05	<0.05	<0.05	<0.05	0.1
Cd	<0.05	0.58	0.27	<0.05	0.71	1.2	0.13	<0.05	5	6
Sb	<0.1	0.82	0.51	0.19	0.65	0.19	0.20	<0.1	4.3	0.85
Te	<0.5	<0.5	<0.5	<0.5	<0.5	<0.5	<0.5	<0.5	<0.1	<0.1
Ba	105	38	46	110	39	78	21	0.6	36	11
Hg	<0.5	<0.5	<0.5	<0.5	<0.5	<0.5	<0.5	<0.5	nd	nd
Tl	<0.05	6.8	11.6	0.2	0.9	4.8	2.5	<0.05	30.0	<10
Pb	0.17	6.1	9.7	0.9	22.6	40.1	4.9	0.14	5	3
Bi	<0.5	<0.5	<0.5	<0.5	<0.5	<0.5	<0.5	<0.5	<0.1	<0.1
U	0.22	3.2	1.8	0.13	0.39	0.17	0.17	0.13	1.3	0.18
$^{87}Sr/^{86}Sr$	0.70759	0.70771	0.70778	0.70803	0.70785	0.70778	0.70778	0.70804	nd	nd

Error on the $^{87}Sr/^{86}Sr$ ratio is 0.00003 ($2 - \sigma$)

nd not determined

The Sr isotopic composition (Table 2) was measured on water samples collected during the 2010 survey. The $^{87}Sr/^{86}Sr$ ranged between 0.70759 and 0.70804, the less radiogenic signature being measured in the sulfurous water sample (RB1). It has to be noted that the Sr isotopic composition in the studied waters spans from the $^{87}Sr/^{86}Sr$ ratio of the Triassic dolostone (0.7076) to limestone (0.7081).

When all of the samples are considered, a positive correlation between the $^{87}Sr/^{86}Sr$ ratio and pH was observed (Fig. 3a). In particular, despite the restricted variability range, the Rio del Lago water samples had lower pH and Sr-isotope ratios downstream of the mine site (samples RB7 and RB5, respectively; $^{87}Sr/^{86}Sr$ from 0.70804 to 0.70778), likely reflecting the admixing of the drainage waters, approaching isotopic equilibrium with the less radiogenic dolostones. The progressive contribution of waters from the dolostone aquifers was also stressed by the negative correlation between the Sr isotopic composition and Mg content (Fig. 3b).

Chemical speciation calculations indicate that all of the samples except TS2 are undersaturated with respect to gypsum, supersaturated with dolomite, and ranged from saturation to supersaturation with calcite. In addition, the TS1 and TS2 samples were supersaturated with hydrozincite, a secondary mineral that is found in the oxidized portions of zinc deposits, and supersaturated with smithsonite, which is produced by the direct oxidation of sphalerite. The TS2 water was also predicted to be slightly undersaturated with malachite, a secondary copper hydroxy carbonate mineral that is commonly produced during the oxidation of copper mineralization at circumneutral pH. Supersaturation with respect to secondary minerals, such as hydrozincite and smithsonite, suggests that the oxidation of sulfide minerals is an active process in the Raibl mine area.

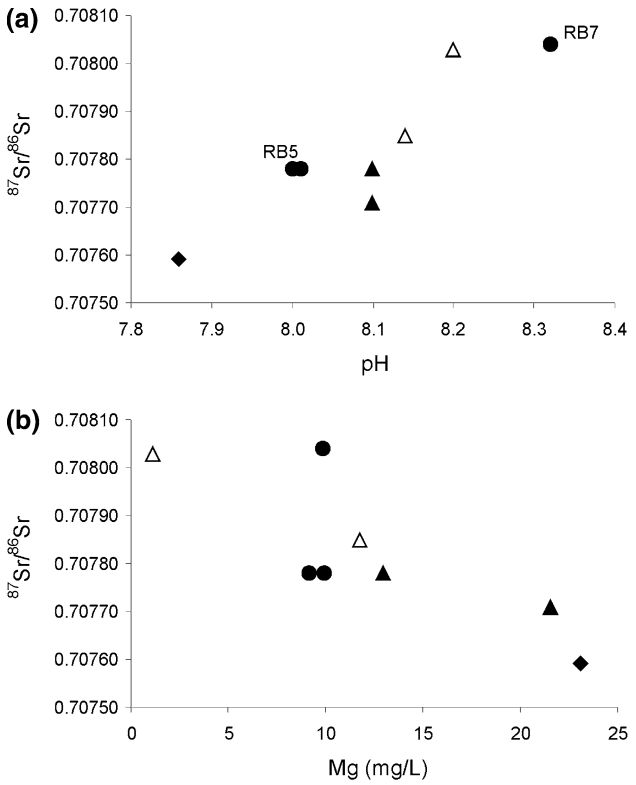

Fig. 3 $^{87}Sr/^{86}Sr$ versus pH (**a**) and $^{87}Sr/^{86}Sr$ versus Mg (**b**) correlation diagrams. *Symbols* as in Fig. 2

The data obtained by this study allows a first pass evaluation of the potential risk posed by drainage from the mine workings and the waste pile on the aquatic ecosystem. As already stressed, drainages and groundwater have an alkaline pH, indicating that the aquifer minerals effectively buffer the acid released by sulfide mineral oxidation. This process affects the transport of dissolved metals, in particular through iron hydroxide precipitation and adsorption of other trace metals and metalloids by this material. However, the data indicate that this effect is different for the various metals. In particular, Tl continues to migrate along groundwater and drainage flow paths and, upon emerging, attains concentrations that pose potential concern for the ecosystem health in the river water and drainage streams, in some cases exceeding guidelines for aquatic ecosystem protection. To evaluate the contribution made by drainage from the mine site on surface water, the upstream concentrations at RB7 can be compared with those downstream at RB5. Water quality data at RB7 indicate contents of dissolved harmful elements are always less than the limits imposed by Italian environmental protection regulations (decree 152/2006).

The concentrations of Mn, Co, Zn, As, Cd, and Sb in surface water increased across the mine setting, but did not exceed the maximum concentration level allowed at the downstream station (RB5). However, Pb and Tl exceeded the thresholds (Fig. 4). The water quality of the drainage samples (TS1 and RB2), which were collected at the same station during the 2006 summer and 2010 winter (Table 2), respectively, also reflects seasonality. This suggests that additional and more detailed surveys are needed to account for seasonal effects and to assess the potential impact on drinking water.

Chemical speciation predictions for the mine drainages indicate that the predominant species present in the Tl-water system should be the Tl(I) ion and, to a much lower extent, $TlSO_4^-$. No solid thallic hydroxide is predicted to form at the pH and Eh of the drainages, supporting the observation that Tl is rather mobile in this system.

Published studies indicate that Tl(I) adsorption on the surface of iron hydroxides is low at low pH and increases at circumneutral conditions (Lin and Nriagu 1998). At Raibl, the relatively high dissolved Tl content, compared for example with As, qualitatively suggests that there is little retention of Tl by ferric hydroxide precipitates. As already

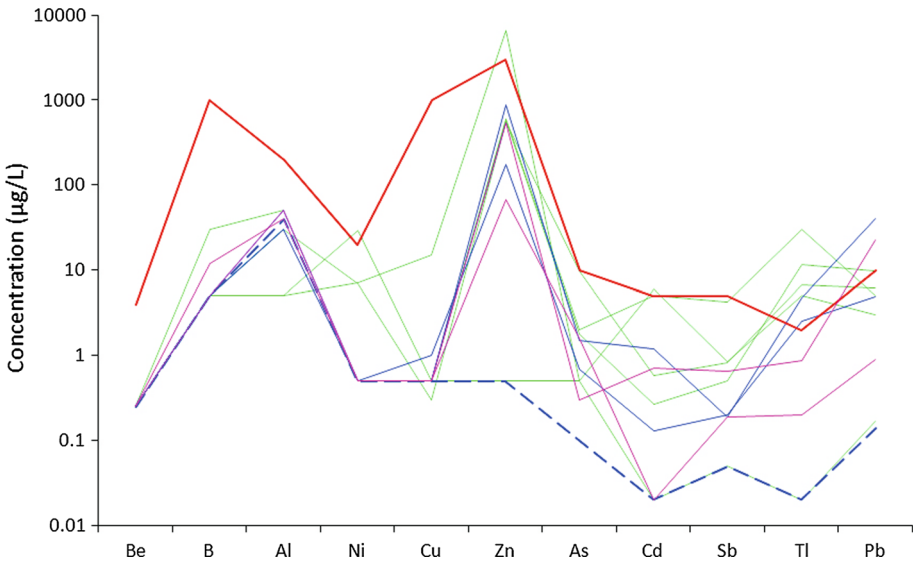

Fig. 4 Elemental patterns for river waters at the mine site (*blue line*); upstream the mine site (*bold-dashed blue line*); springs (*pink line*); drainages (*green line*); maximum admissible water quality thresholds for environmental protection in Italy (*bold red line*)

stated, it is known that manganese dioxide has a strong adsorptive power for Tl; however, on the basis of the Eh–pH and the other dissolved species, it can be predicted that rhodochrosite ($MnCO_3$) precipitation is promoted from the studied waters, lowering the dissolved Mn concentrations but not significantly scavenging Tl from solution.

The use of Sr isotope ratios allowed the potential hydrogeochemical and exchange processes operating along water flow paths in the carbonate host rocks to be evaluated. Changes in the $^{87}Sr/^{86}Sr$ ratio over distance due to isotopic gradients during advective flow may be expressed through the Damköler number (N_D) (e.g. Blattner and Lassey 1989). Assuming an isotope-ratio of the total dissolution flux from the solid of 0.7077, i.e. supposing that the mineralization process was not accompanied by significant changes in the Sr isotopic composition with respect to the hosting dolostone, and an initial isotope ratio of 0.7081 (the isotopic signature of limestone), the Sr-isotopic variations measured in the Raibl waters can be simulated by a velocity of 2.0 m/year, a reaction rate of 1E−6, and a system length of about 1500 m, with a N_D value of 9.0. The high N_D value, expected for advection-limited systems, implies that the reaction kinetics are rapid as compared to the rate of solute transport. In addition, the low water velocity indicates that the circulation occurs in porous media rather than in discrete fractures. Furthermore, assuming a near-conservative behavior for Tl and an initial concentration of 30 µg/L, the highest value measured in drainages, for the source zone, the observed $^{87}Sr/^{86}Sr$ versus Tl correlation can be roughly simulated (Fig. 5).

Thallium released by oxidation of host sulfide minerals and transported through drainage water and surface water may be sorbed by soils (Jacobson et al. 2005) and mine wastes, becoming potentially bioavailable to plants

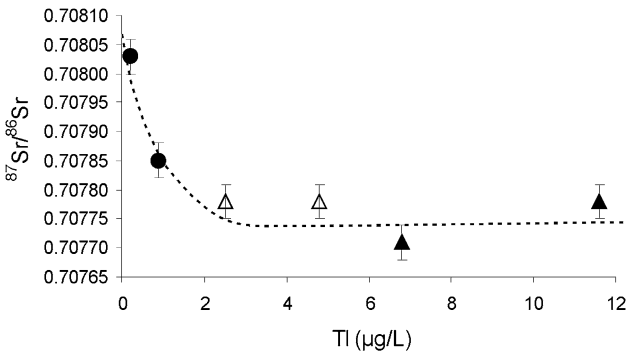

Fig. 5 $^{87}Sr/^{86}Sr$ versus Tl concentration correlation diagram. The *dashed line* represents the coupled water–rock reaction and mixing patterns (see text for explanations)

growing in these materials. In particular, Tl hyperaccumulation has been measured in metallophytes belonging to the *Thlaspietum cepaeifolii* plant community growing in native and mine soils, mine tailings, and stream banks at the Raibl mine site (Fellet et al. 2012).

Conclusions

The geochemistry of mine effluents, springs, and surface water was investigated at the Raibl mine site (Cave del Predil) in the southeastern Alps. After the mine was closed, the underground workings flooded; at present, drainages return a significant amount of impacted water to the surface waterway. The data reveal that sulfide weathering is occurring at Raibl, even if the produced acidity is buffered by the carbonate host-rocks. The pH changes drive extensive iron hydroxide precipitation, lowering the content of most of the harmful elements to below the thresholds imposed

for aquatic environmental protection by Italian regulations. However, Tl concentrations that exceeded the maximum permissible concentration were observed at the downstream sampling station. Most significantly, Tl at concentrations of concern were measured in the valley stream water despite the strong effects of dilution by uncontaminated tributaries. This suggests that this element is not significantly scavenged by iron hydroxide precipitation. The data also indicate seasonal water chemistry effects. More detailed investigations are warranted to better evaluate the fate of Tl in the water–sediment-soil system at Cave del Predil, including its possible effects on the aquatic ecosystem and on the water resources commonly used by local communities.

Acknowledgments L. Zini helped during the field survey; A. Lutman and S. Pison are thanked for discussions. The authors also wish to thank one of the referees, whose critical comments and careful revision greatly improved the manuscript.

References

Alderton DHM, Serafimovski T, Mullen B, Fairall K, James S (2005) The chemistry of waters associated with metal mining in Macedonia. Mine Water Environ 24:139–149

Allison JD, Brown DS, Novo-Gradac KJ (1991) MINTEQA2/PRODEFA2, a geochemical assessment model for environmental systems. U.S. EPA report 600/3-91/021, Washington DC

ATSDR (2014) Agency for toxic substances and disease registry. Health Consultation, Utah Dept of Health, http://www.atsdr.cdc.gov/HAC/pha/TraverseMountainHC/Traverse_Mountain_HC_PC_07-07-2014.pdf

Bidoglio G, Gibson PN, O'Gorman M, Roberts KJ (1993) X-ray adsorption spectroscopy investigation of surface redox transformations of thallium and chromium on colloidal mineral oxides. Geochim Cosmochim Acta 57:2389–2395

Blattner P, Lassey KR (1989) Stable-isotope exchange fronts, Damköler numbers and fluid to rock ratios. Chem Geol 78:381–392

Brigo L, Omenetto P (1979) The lead and zinc ores of the Raibl (Cave del Predil-northern Italy) Zone: new metallogenic data. Verh Geol Bundesaust 3:241–247

Brigo L, Kostelka L, Omenetto P, Schneider HJ, Schroll E, Schulz O, Strucl I (1977) Comparative reflections on four Alpine Pb-Zn deposits. In: Klemm DD, Schneider HJ (eds) Time- and stratabound ore deposits. Springer, Berlin, pp 273–293

Cerny L (1989) Current prospecting strategy for carbonate-hosted Pb–Zn mineralizations at Bleiberg-Kreuth (Austria). Econ Geol 84:1430–1435

Cidu R (2011) Mobility of aqueous contaminants at abandoned mining sites: insights from case studies in Sardinia with implications for remediation. Environ Earth Sci 64:503–512. doi:10.1007/s12665-010-0874-y

Cidu R, Dadea C, Desogus P, Fanfani L, Manca PP, Orrù G (2012) Assessment of environmental hazards at abandoned mining sites: a case study in Sardinia, Italy. Appl Geochem 27:1795–1806

Ebner F, Cerny I, Eichhorn R, Götzinger M, Paar WH, Prochaska W, Weber L (2000) Mineral resources in the Eastern Alps and adjoining areas. Mitt Österr Geol G 92:157–184

Fellet G, Pošćić F, Casolo V, Marchiol L (2012) Metallophytes and thallium hyperaccumulation at the former Raibl lead/zinc mining site (Julian Alps, Italy). Plant Biosyst 146:1023–1036

Foley NK (2002) Environmental geochemistry of platform carbonate-hosted sulfide deposits. In: Seal RR, Foley NK (eds) Progress on geoenvironmental models for selected mineral deposit types. USGS OFR 02-195, Denver CO, USA

Jacobson AR, McBride MB, Baveye P, Steenhuis TS (2005) Environmental factors determining the trace-level sorption of silver and thallium to soils. Sci Total Environ 345:191–205

Jambor JL, Blowes DW, Ritchie AIM (eds) (2003) Environmental aspects of mine wastes. Mineralogical Assoc of Canada Short Course Series vol 31, ISBN-13:978-0921294313

Kaplan DI, Mattigod SV (1998) Aqueous geochemistry of thallium. In: Nriagu JO (ed) Thallium in the Environment. Wiley-Interscience, London, pp 15–29

Kelley KD, Leach DL, Johnson CA, Clark JL, Fayek M, Slack JF, Anderson VM, Ayuso LE, Ridley WI (2004) Textural, compositional and sulfur isotope variations of sulfide minerals in the Red Dog Zn–Pb–Ag deposits, Brooks Range, Alaska: implications for ore formation. Econ Geol 99:1509–1532

Koschinsky A, Hein JR (2003) Uptake of elements from seawater by ferromanganese crusts: solid-phase association and seawater speciation. Mar Geol 198:331–351

Law S, Turner A (2011) Thallium in the hydrosphere of south west England. Environ Poll 159:3484–3489

Leach DL, Viets JB, Foley-Ayuso N, Klein DP (1995) Mississippi valley-type Pb–Zn deposits. In: du Bray EA (ed) Preliminary compilation of descriptive geoenvironmental mineral deposit models. USGS OFR 95-831:234–243

Leach DL, Sangster DF, Kelley KD, Large RR, Garven G, Allen CR, Gutzmer J and Walters S (2005) Sediment-hosted lead-zinc deposits: a global perspective. Econ Geol 105:561–607. http://alaska.usgs.gov/staff/geology/bradley/pubs/2010_Leach_secular_Pb-Zn.pdf

Leach DL, Bradley DC, Huston D, Pisarevsky SA, Taylor RD, Gardoll SJ (2010) Sediment-hosted lead-zinc deposits in Earth history. Econ Geol 105:593–625

Lin T-S, Nriagu JO (1998) Revised hydrolysis constants for thallium(I) and thallium(III) and the environmental implications. J Air Waste Manage Assoc 48:151–156

Luoma SN, Rainbow PS (2008) Metal contamination in aquatic environments. Cambridge University Press, Cambridge

Martinez-Frías J (1991) Sulphide and sulphosalt mineralogy and paragenesis from the Sierra Almagrera veins, Betic Cordillera (SE Spain). Estudios Geol 47:271–279

Mulkey JP, Oehme FW (1993) A review of thallium toxicity. Vet Human Toxicol 35:445–453

Murao S, Itoh S (1992) High thallium content in Kuroko-type ore. J Geochem Explor 43:223–231

Nordstrom DK (1977) Thermochemical redox equilibria of ZoBell's solution. Geochim Cosmochim Acta 41:1835–1841

Nordstrom DK (2011) Hydrogeochemical processes governing the origin, transport and fate of major and trace elements from mine wastes and mineralized rock to surface waters. Appl Geochem 26:1777–1791

Nriagu JO (1998) Thallium in the environment. Wiley, New York City

Parkhurst DL, Appelo AAJ (1999) User's guide to PREEQC (version 2)—a computer program for speciation, batch-reaction, one dimensional transport, and inverse geochemical modeling. USGS, p 99-4259

Peter AL, Viraraghavan T (2005) Thallium: a review of public health and environmental concerns. Environ Int 31:493–501

Plumlee GS, Smith KS, Montour MR, Ficklin WH, Mosier EL (1999) Geologic controls on the composition of natural waters and mine

waters draining diverse mineral-deposit types. In: Filipe LH, Plumlee GS (eds) The environmental geochemistry of mineral desposits: case studies and research topics. Rev Econ Geol 6B: 373–432

Sager M (1994) Thallium. Toxicol Environ Chem 45:11–32

Schroll E (1996) The Triassic carbonate-hosted Pb–Zn mineralization in the Alps (Europe). The metallogenetic position of Bleiberg type. In: Sangster DF (ed), Carbonate-hosted lead–zinc deposits. Soc Econ Geol Spec Publ 4: 182–194

Schroll E, Prochaska W (2004) Contribution to ore fluid chemistry of Bleiberg Pb–Zn deposit (Austria) and affiliated deposits. Geochim Cosmochim Acta Suppl, Abstracts, 13th V.M. Goldschmidt Conf, A306

Schroll E, Rantitsch G (2005) Sulfur isotope patterns from the Bleiberg deposits (eastern Alps) and their implications for genetically affiliated lead-zinc deposits. Mineral Petrol 85:1–18

Smith KS, Huyck HLO (1999) An overview of the abundance, relative mobility, bioavailability, and human toxicity of metals. In: Plumlee GS, Logsdon MJ (eds) The environmental geochemistry of mineral deposits: part A. Processes, techniques and health issues, Rev Econ Geol 6A: 29–70

Xiao T, Guha J, Boyle D, Liu C-Q, Zheng B, Wilson GC, Rouleau A, Chen J (2004) Naturally occurring thallium: a hidden geoenvironmental hazard? Environ Int 30:501–507